Journal of African Earth Sciences 138 (2018) 192–200

Contents lists available at ScienceDirect

Journal of African Earth Sciences

journal homepage: www.elsevier.com/locate/jafrearsci

Coastal dynamics of uplifted and emerged late Pleistocene near-shore coral patch reefs at fins (eastern coastal Oman, Gulf of Oman)

Frank Mattern [a,*], Daniel Moraetis [a], Iftikhar Abbasi [a], Bushra Al Shukaili [a], Andreas Scharf [a], Michel Claereboudt [b], Elayne Looker [c], Nihal Al Haddabi [a], Bernhard Pracejus [a]

[a] Department of Earth Sciences, College of Science, Sultan Qaboos University, P.O. Box: 36, PC 123, Al-Khod, Muscat, Oman
[b] Department of Marine Science and Fisheries Agricultural and Marine Sciences, Sultan Qaboos University, P.O. Box: 36, PC 123, Al-Khod, Muscat, Oman
[c] Five Oceans Environmental Services LLC, P.O. Box: 660, PC 131, Muscat, Oman

ARTICLE INFO

Article history:
Received 27 August 2017
Received in revised form
13 November 2017
Accepted 16 November 2017
Available online 17 November 2017

Keywords:
Coral patch reefs
Weichselian
Holocene sea-level
Uplift rate and stages
Marine terraces
Diagenesis

ABSTRACT

We investigated two coral patch reefs of probably Weichselian age (Wyns et al., 1992a) which have been uplifted above sea-level in the coastal setting of uplifted marine terraces adjacent to the Oman Mountains. Uplift is also manifested in raised beach conglomerates and a wave-cut notch. We document some of the main reef features in the apprehension that building/development will preclude the study of the reefs in the near future. The reefs formed above a hardground of bioclastic limestone (mudstone to wackestone), characterized by intense bioerosion and red algae. The red algae may occur so plentiful to form (very localized) bafflestones. The diagenetic history of the rocks includes a transition from a marine environment (first cement) to meteoric conditions (dissolution and second cement). The reefs are 1.5 m thick and display planar as well as gently ocean-dipping reef tops, suggesting exposure to the wave-cut activity and, thus, shallow and nearshore deposition. The reefs are dominated by one coral species, identified as *Cyphastrea serailia*. On the protected side of the reefs the corals developed wavy and columnar growth forms while on the ocean facing side irregularly shaped exoskeletons developed. Our GPS-based topographic survey revealed an elevation of the two reefs of 21.5 m ± 0.06 m above sea-level. Taking into account (1) the global Holocene sea-level rise of 120 m ± 20 m (Pirazzoli and Pluet, 1991), (2) formation of the reefs slightly below sea-level (~1.5 m) as well as (3) their present position above sea-level, we quantify the total upward transfer of the reefs to be 143 m and the average uplift rate to be 6.8 or 4.6 mm/yr depending on the correct age (either ~21,000 or ~31,000 yr B.P.). As the causes of uplift we mainly consider isostatic rebound following the late Cretaceous formation of the Oman Mountains (Yuan et al., 2016). The terrace development went through the following stages: (1) The patch reefs formed in shallow water. (2) Initial, gentle uplift caused abrasion of the reef tops. (3) Uplift continued and beach conglomerate 1was deposited on top of the reefs. (4) Abrasion continued, creating an abrasion platform. Uplift and creation of borings in platform required time and an interval of relatively slow uplift and tectonically and climatically stable conditions. (5) Uplift took place, and a wave-cut notch formed below the reefs. (6) Notch formation, including the borings into the notch, required time and stable conditions and was followed by deposition of beach conglomerate 2. (7) Finally, emergence/exposure of the notch and conglomerate 2 above sea-level ensued due to pronounced uplift, possibly associated with faulting and earthquakes. Formation of the reefs and the abrasion platform can be correlated with MIS 3 (Marine Isotope Stage 3) and notch formation with MIS 1.

1. Introduction

The investigated reefs near Fins (Fig. 1A) have previously not been studied in detail. They have been mapped as part of the Quaternary, “subrecent” marine limestone unit “Qmy” (Fig. 1B) that

* Corresponding author.
E-mail address: frank@squ.edu (F. Mattern).

https://doi.org/10.1016/j.jafrearsci.2017.11.018
1464-343X/

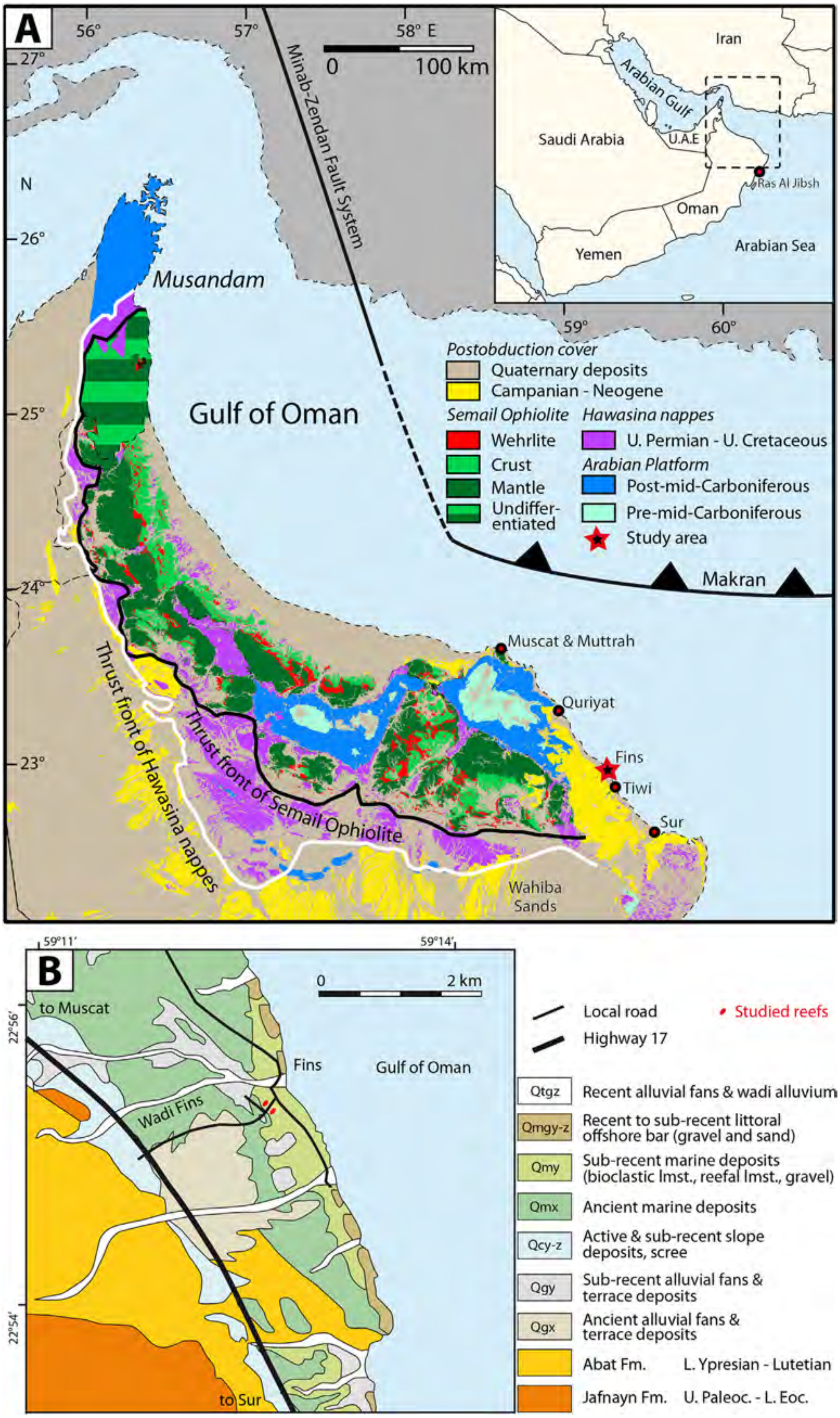

Fig. 1. Study area. (A) Geological map of the Oman Mountains and position of the study area at Fins, slightly modified after Béchennec et al. (1993). (B) Geological map of the study area, drawn after (Wyns et al., 1992b). For easier identification the two studied reefs are shown in red and slightly increased in size. (For interpretation of the references to colour in this figure legend, the reader is referred to the web version of this article.)

extends to the ocean (Fig. 1B) where it forms a cliff. The related geological description of this unit is very brief. All that is mentioned by (Wyns et al., 1992a) is that the "Qmy unit" comprises bioclastic as well as reefal limestone. The latter contains corals and calcareous algae and is overlain by a marine conglomerate (Wyns et al., 1992a). The conglomerate has been analyzed by Al Haddabi (2015) in the course of a beachrock study of the Fins/Tiwi area. Only recently, the reefs of the reefal limestone have been described in detail by Al Shukaili (2015). Her results and other data are the subject of this article. The monograph on "Reef corals and coral reefs of the Gulf of Oman" by Claereboudt (2006) provided significant orientation in describing the reefs and in classifying the corals.

According to Wyns et al. (1992a), the "Qmy unit" forms a marine terrace at an elevation between 10 and 20 m. They correlated this terrace with marine deposits occurring at an elevation of 12–15 m close to Ras al Jibsh (Fig. 1A), east of the Wahiba Sands, which have been dated by the ^{14}C method as 21,280 ± 280 yr B.P and 31,110 ± 530 yr B.P. on mollusk shells by Gardner (1988). Moreover, Wyns et al. (1992a) also correlate the "Qmy unit" with deposits of a drillhole core from Muttrah near Muscat. This core revealed a high sea-level at 31,890 ± 765 yr B.P. (Hannss, 1991, in Wyns et al., 1992a). Based on these ages, Wyns et al. (1992a) assigned a Weichselian age to these marine deposits. The Weichselian designates the last glacial period of the Pleistocene glaciation, when the global sea-level was 120 m (±20 m, according to most estimates) lower than today, approximately 21,000 yr B.P. (Pirazzoli and Pluet, 1991; see also Siddall et al., 2003).

Uplift of Quaternary marine terraces above sea-level may measure 190 m in the Tiwi/Fins area (Kusky et al., 2005). Northern Oman has active fault systems that accommodate uplift (Kusky et al., 2005). The fact that the Arabian Plate underrides Eurasia in the north (Iranian sector) may create a forebulge where the Fins/Tiwi area is located and bulging may be responsible for the uplift (Kusky et al., 2005). For more details on the geology of the marine terraces of the Fins/Tiwi area the reader is referred to the regional studies of Kusky et al. (2005), Hoffmann et al. (2013) and Yuan et al. (2016).

Since there are no details on the reefs of the "Qmy unit" available, we intend to contribute to their understanding by a geomorphological characterization of two small reefs (Fig. 1), determination of the coral species, the description of their growth forms and ecology. This takes place against the backdrop of increasing building development which is affecting the marine terraces of the Fins/Tiwi area as they represent sought after building sites with special consideration of the proximity of the rapidly expanding community of Fins (Fig. 1). These aspects could very soon lead to the disappearance of the reefs. Thus, there is some urgency to document the above mentioned reef features before the reefs will be lost. Since the reefs are situated on a marine terrace it is of interest to know their exact elevation which we determined.

After outlining the external features of the reef and determining their elevation we will describe the different lithologies as well as the reefs. We will then interpret a few details of our lithological observations and put forward a sequence of relevant depositional and erosional processes as well as a quantification of the total upward reef transfer (uplift) and the average annual uplift rate. Following a correlation of observed features with the Marine Isotope Stages (MIS; Siddall et al., 2003) we will discuss main causes for uplift.

We define a patch reef as a small, isolated carbonate build-up with platform character (table reef). The surface of near-shore patch reefs may exhibit a gentle seaward dip. Patch reefs are small-scale reef versions of standard reef types (e.g., fringing reefs, barrier reefs). They stand a few meters high (commonly 3–6 m) above the surrounding ground and have a diameter of 5–50 m. Regarding the ecology and sedimentary architecture of patch reefs the interested reader is referred to Mazzulo et al. (1992).

2. Study area and geological setting

The two studied small reefs are located SSW of the nearby coastal community of Fins (Fig. 1) within the Sharqiyah region of northeastern Oman, 100 km southeast of Muscat. The coordinates of the northwestern and southeastern reefs are 22°55′15.95″N/59°12′34.24″E and 22°55′13.79″N/59°12′35.97″E, respectively. The reefs are easily accessible by a road (Fig. 2A).

The geological setting of the reefs is a narrow coastal zone which strikes northwest-southeast and is characterized by the occurrence of Quaternary marine terraces (Wyns et al., 1992a, b; Kusky et al., 2005; Hoffmann et al., 2013; Yuan et al., 2016). The terraces occur in Paleogene rocks in the southwest and in Quaternary rocks to the northeast, i.e. towards the shore (Fig. 1). Marine terraces are uplifted wave-cut/abrasion platforms (see Trenhaile, 2000). Wave-cut action is indicated by their gentle oceanward dip and their association with wave-cut notches (for notch formation see Cooper et al., 2007). The studied coastal segment is characterized by mesotidal conditions (compare Short, 1991). Pluvial periods occurred from 6000 to 10,500 and 78,000 to 82,000 yr B.P. (Fleitmann et al., 2003).

The Paleogene rocks are mainly carbonates, consisting of hard, compact foraminiferal limestone, interbedded with a few shale beds and calcareous sandstone. They are exposed over a large area along the Tiwi-Quriyat coastal belt on the northern flank of the Oman Mountains (Glennie et al., 1974; Wyns et al., 1992a).

The Oman Mountains comprise a complex assemblage of kilometer-scale, thick, siliciclastic and carbonate rocks of Precambrian to Neogene age. Thick Permian-Cretaceous autochthonous carbonate rocks were deposited along the Tethys margin and thrust over by allochthonous oceanic mantle and crust including ocean floor sediments belonging to the Semail Ophiolite and Hawasina Supergroup, respectively. The allochthonous sheets were thrust from the northeast due to closure of the Tethys Ocean during Late Cretaceous time (Glennie et al., 1973, 1974; Searle and Malpas, 1980; Lippard et al., 1986; Searle and Cox, 1991; Hacker et al., 1996; Goffé et al., 1988; Glennie, 2005; Rollinson et al., 2014). Postobduction carbonate sedimentation resumed since the late Cretaceous and continued until the Miocene in the study area.

The study area was uplifted during the Cenozoic and parts of the Semail Ophiolite and the underlying rocks have been exhumed (Searle, 2007). Also during the Cenozoic, the Arabian Plate started to collide with the Eurasian Plate, forming the Zagros Mountains (Searle, 2007). Since then the Arabian Plate is being subducted along the Makran Coast (Harms et al., 1984; Wiedicke et al., 2001). The study area may have been uplifted as part of the forebulge associated with the collision (Kusky et al., 2005). The area is seismically active with very low-magnitude earthquakes (Kusky et al., 2005).

3. Methods

Our study relies on field work, including field description of the reefs and sampling, as well as a topographic survey of the Fins/Tiwi area which included the reefs. We also studied the facies of the bioclastic limestone in thin section.

The topographic survey was performed with a double precision Real Time Kinematic (RTK) GPS receiver (Trimble) and it was readily corrected to provide coordinates under the reference points supplied by the National Survey Authority of the Sultanate of Oman. The topographic dataset includes a total of 369 survey points, measured under an excellent geometric dilution of precision

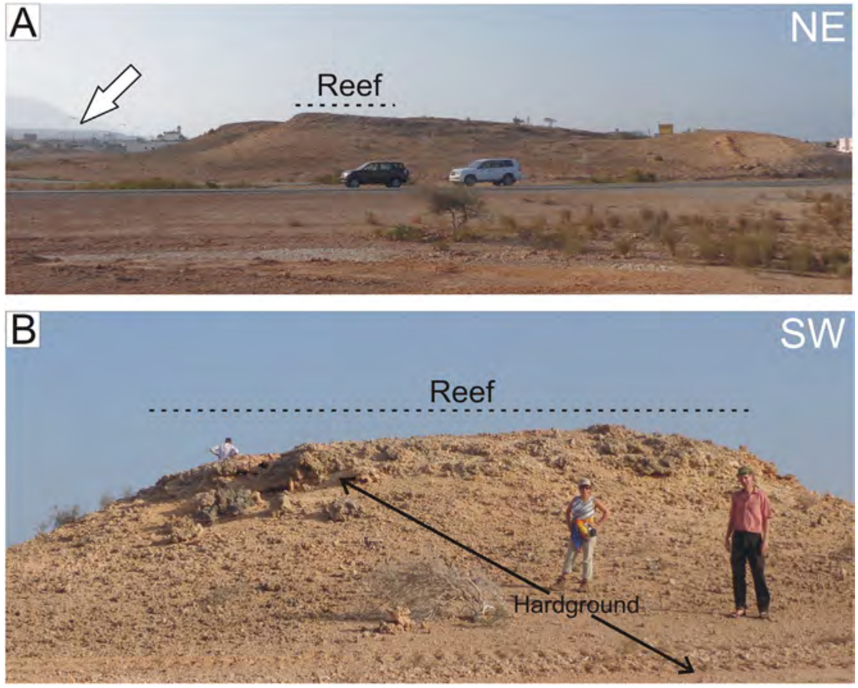

Fig. 2. Side views of the two studied reefs. The horizontal dashed lines indicate the lateral extent of the reefs. Note the gentle dip of both reef tops to the northeast! Also note that the reefs tower a few meters above the surrounding deposits as they are resting on a "pedestal" of bioclastic limestone! (A) Northwestern reef. The view is to the northwest. The vehicles are standing on the marine terrace marked by the "Qmy unit". The surface of the terrace seen in the foreground is a bored hardground. Also note marine terrace in the background (arrow)! (B) Southeastern reef. The view is to the southeast. The two scale persons stand on the surface of the marine terrace which is a bored hardground. The scale person on the right is two meters tall.

(GDOP) and accuracy of <1 cm. The topographic survey took place on two days, on October 31st and November 28th, 2015 between 13:00 to 17:00 h. For the tide fluctuations of these two days see Table 1.

4. Results

The lithostratigraphy can be easily summarized. A few meters (>5 m) of bioclastic limestone is overlain by coral patch reefs which measure 1.5 m in thickness. Both reefs are overlain by a few decimeters of conglomerate (conglomerate 1). Another beach conglomerate (conglomerate 2) is cemented onto a wave-cut notch occurring within the bioclastic limestone. The conglomerates formed at different vertical/stratigraphic positions.

The two reefs have a long axes of 20 m and 15 m, respectively (Fig. 2A and B). Across their long axes they measure 10–15 m. The reefs are 1.5 m thick and overtop the surrounding deposits by a few meters (Fig. 2) as they rest on a "pedestal" of bioclastic limestone (Fig. 2 A, B). Both reefs display an inclined surface that gently dips towards the ocean which is to the northeast (Fig. 2) like the marine terraces of the region. Thus, the ocean-facing forereef areas which are located on the northeastern parts of the reefs have been built in slightly deeper water than those parts of the reefs that were more protected on the landward sides.

At the shore, just northeast of the reefs, we observed a wave-cut notch in the bioclastic limestone and the clast-supported beach conglomerate 2 with well-rounded pebble clasts within the "Qmy unit", both situated well above the sea-level (Fig. 3A). Thus, both phenomena provide additional and independent evidence for the uplift of the "Qmy unit" besides the evidence offered by the reefs. The conglomerate 2 was deposited into the notch (Fig. 3A). The notch surface displays a multitude of borings by unidentified organisms. Erosion of the notch was not only due to wave action, as indicated by countless borings (Fig. 3B). Borings are a striking feature of the bioclastic limestone.

Fig. 4A shows the bioclastic limestone which represents the surface of the marine terrace and which is littered by mainly shallow borings (Fig. 4A), indicating that this surface represents a hardground. At least some of the borings were caused by bivalves. The evidence for this is the presence of a bivalve within one of the borings found in the bioclastic limestone (Fig. 4B). There are also borings by the sponge *Cliona* sp. As encrusting and sessile organisms corals need hardgrounds to attach their exoskeletons (e.g., Flügel, 2010: p. 208) to form colonies/reefs. Accordingly, Fig. 4C shows the bored hardground of the bioclastic limestone directly overlain by corals. Evidently, the hardground stretches from the surface of the marine terrace to the base of the reef (compare Fig. 2B with Fig. 4).

Table 1
The tide fluctuations for October 31st and November 28th, 2015 between 13:00 to 17:00 h for Muscat (Oman): 23.6167°N, 58.6000°E.

Day	High tides	Low tides	Sunrise	Sunset
Oct. 31st	12:14 AM GST 2.89 m	5:58 AM GST 1.43 m	6:10 AM GST	5:27 PM GST
Oct. 31st	11:22 PM GST 2.59 m	6:06 PM GST 0.48 m		
Nov. 28th	10:19 AM GST 2.62 m	4:58 AM GST 1.43 m	6:28 AM GST	5:18 PM GST
Nov. 28th		5:01 PM GST 0.29 m		

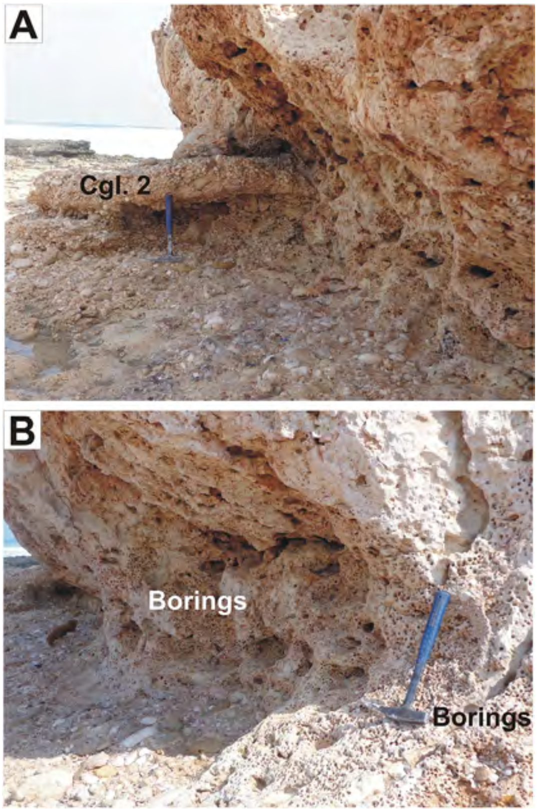

Fig. 3. The “Qmy unit” close to shore. (A) The view is to the north and shows in the background the contact of the “Qmy unit” with the sea in the form of a vertical cliff. In the foreground on the right side, the bioclastic limestone of the unit displays a wave-cut notch. Notch formation was followed by deposition of the local beach conglomerate 2 which is cemented onto/into the notch vertically and laterally. Both, the notch and the beach conglomerate provide evidence for the uplift of the “Qmy unit” above the sea-level. (B) “Qmy unit” in the same outcrop as in A. The bioclastic limestone that forms the notch displays a multitude of borings, indicating significant bioerosion.

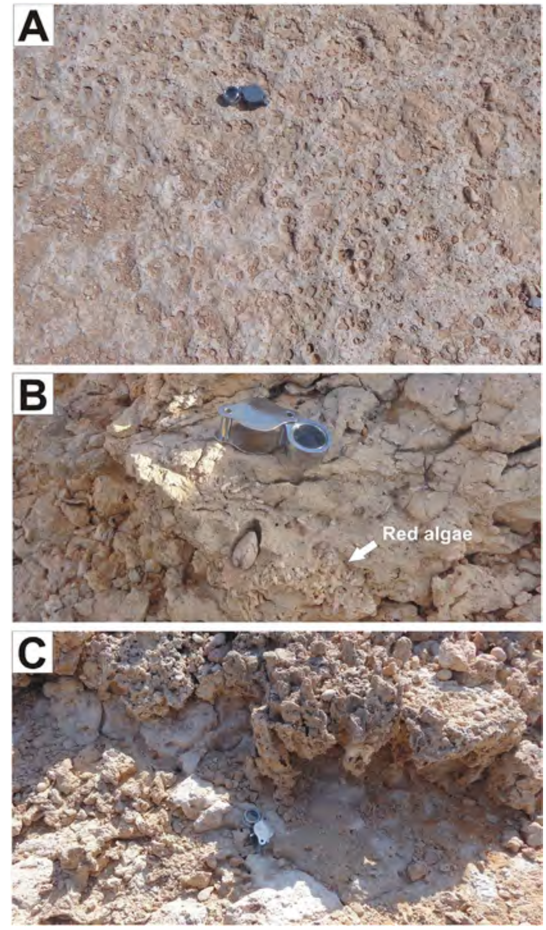

Fig. 4. Bored hardgrounds of the bioclastic limestone of the “Qmy unit”. (A) Surface of the marine terrace is covered by borings which are mainly shallow. (B) Bivalve as a boring organism preserved in its own boring below the hand lens. Note the shape match between boring and bivalve! Also note red algae (rhodoliths; light color)! C. Corals directly overlying the hardground. Note borings to the right of the hand lens!. (For interpretation of the references to colour in this figure legend, the reader is referred to the web version of this article.)

The bioclastic limestone contains well-developed red algae (rhodoliths) which can be identified with the naked eye or with a hand lens (for rhodoliths see McCoy and Kamenos, 2015; Aguirre et al., 2017; see Fig. 4B). Under the microscope the bioclastic limestone, directly underlying the reefs, is classified as a mudstone to wackestone sensu Dunham (1962). The micritic to microsparitic matrix supports fragments of red algae, corals, small bivalves, echinoid with syntaxial overgrowth, monaxon sponge spicules (some made of silica, some made of calcium carbonate) and bryozoans (?). The vuggy pores of a dissolved coral are partly filled with equant, drusy calcite cement (Fig. 5).

In some parts of the bioclastic limestone, red algae are so abundant that they represent rock formers. The branching style of the algae may be particular as the angle of the branching twigs is minimal (acute angle), that a system of subparallel and even parallel oriented twigs is created. These local parts of the reefal limestone are classified as algae bafflestones sensu Embry and Klovan (1971). In thin sections perpendicular to the algae twigs the algae display fine-scale cells of the hypothallus forming a cellular pattern or latticework with concentric and radial aspects. The exterior perithallus is partly well-developed with aligned conceptacles. The algae constitute 50% of the bafflestones.

Besides the algae, there is fine-grained matrix (mainly microsparite, some micrite), supporting angular quartz grains, representing very fine sand as well as 10–15% of the primary detritus. Other matrix components are mafic mineral grains that are smaller, better rounded and fewer compared to the quartz grains as well as occasional sand-size micrite clasts and vein calcite clasts. The carbonate clasts are angular and may exceed the size of the quartz grains but are fewer. We found no definite bioclasts in the matrix.

The bafflestones also exhibit growth framework porosity sensu Choquette and Pray (1970). At their margins, some red algae show a radial pattern of elongate pores that are widening outward and classify as shrinkage crack pores in the sense of Choquette and Pray (1970). Both pore types display thin linings of microcrystalline cement of calcium carbonate. The conceptacles may display the same feature. Among the conceptacles, however, the microcrystalline cement may be followed by a second generation of cement which consists of larger (and equant) crystals of calcium carbonate, providing for drusy mosaics of the pore fillings (Fig. 6). There is no indication for dissolution-related pores.

The beach conglomerates 1 and 2 are light-colored (commonly beige), poorly sorted, well-rounded, clast-supported and polymictic, exhibiting different limestone clasts, vein quartz and quartzite fragments as well as clasts of igneous rocks. These clasts are pebble-sized.

The corals of the reefal limestone belong to the family of the *Faviidae*. Most of the samples we collected definitely belong to the genera *Cyphastrea*. They form massive or encrusting colonies with

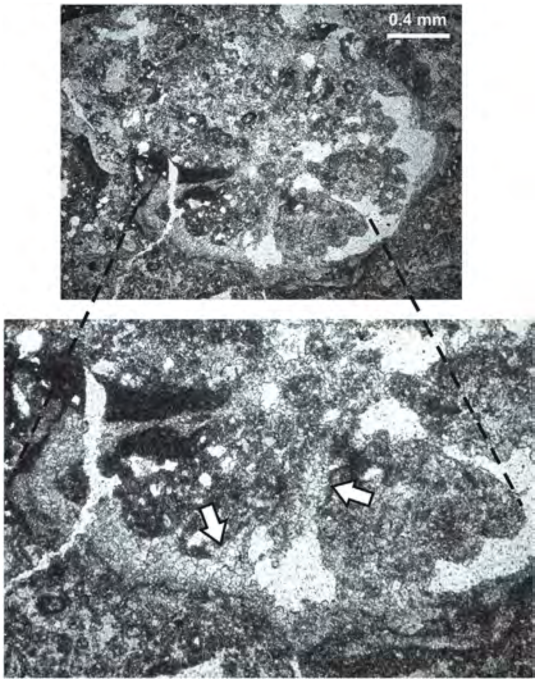

Fig. 5. Thin section photomicrograph of dissolved coral (top, overview). Detail below shows vuggy pores, partly filled with equant, drusy calcite cement (arrows). Bioclastic limestone (mudstone to wackestone). Plane polarized light.

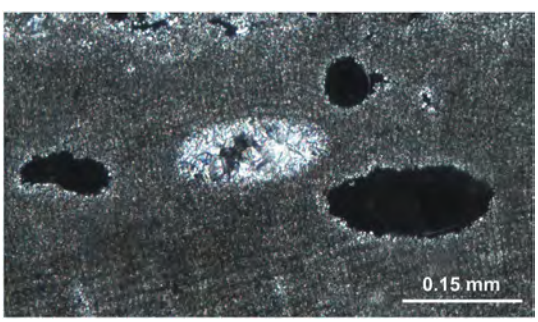

Fig. 6. Thin section photomicrograph of a marginal part of a red algae with conceptacles. The conceptacles on the left and on the right are lined with thin microcrystalline calcium carbonate cement (first generation of cement). The conceptacle in the center, however, also displays larger and equant crystals of calcium carbonate, providing for a drusy mosaic of the pore filling (second generation of cement). Crossed polarized light. (For interpretation of the references to colour in this figure legend, the reader is referred to the web version of this article.)

short branches. Their corallites are typically plocoid with calices not exceeding 4 mm in diameter. A columella is usually present. Costae are well developed but limited to the wall of the corallites. Septa, costae and the coenosteum are finely granulated (for terminology see Claereboudt, 2006).

Almost all *Cyphastrea* samples belong to the species *serailia* (*Cyphastrea seralia* FORSKÅL 1775), containing 12 primary septa, and the secondary septa are usually poorly developed (Claereboudt, 2006). The corallites are subequal in size and rounded. These are a few of the most distinctive features of this species. Generally, the colonies of *Cyphastrea seralia* are massive or columnar, and the surface of the colonies is hillocky (Claereboudt, 2006). Around the Gulf of Oman this species is less common than *Cyphastrea microphtalma*, but it can be found in most reef environments (Claereboudt, 2006). *Cyphastrea seralia* is more abundant in protected turbid environment where both *Cyphastrea microphtalma* and *Cyphastrea seralia* are relatively common (Claereboudt, 2006). In the outcrop their color is usually pale grey. Only one coral species is dominating the reefs at Fins.

In general, the corals are mainly massive with a few of them having a domal shape. Corals on the slightly shallower and protected, landward side of the reefs display different growth forms from those at the slightly deeper, ocean facing side. Whereas the corals on the protected side developed wavy and columnar growth forms (Fig. 7A and B) corals on the ocean facing side developed irregularly shaped exoskeletons (Fig. 7C). On both sides calcified red algae (rhodoliths) occur, probably belonging to the genus *Lithothamnion*.

Among the reefs we found bivalves, and the reef top is associated with encrusted serpulid worm tubes. The corals may be bored. On the floor, surrounding the reefs, that is overtopped by the reefs we noticed lose fossil bivalve shells (not modern shells) belonging to the *Pteriomorphia*, e.g., *Chlamys*, *Pecten*. These bivalves occur as isolated shells or as parts of limestone cobbles. The significance of their occurrence is unclear as they are not part of the outcrops.

Our topographic survey revealed the elevation of the two reefs to be 21.5 m $\pm$ 0.06 m above sea-level. Thus, their elevation exceeds the value of 10–20 m as determined for the “Qmy unit” by Wyns et al. (1992a). The exact determination of the elevation of the reefs is one prerequisite to quantify the amount of uplift as well as the uplift rate of the reefs. When the last glaciation was at its maximum, approximately 21,000 years ago, the global sea-level was much lower than today ($-$120 m $\pm$ 20 m, according to most estimates, e.g. Pirazzoli and Pluet, 1991). Melting of the ice caps caused the global sea-level to rise at rates possibly as high as 20 mm/yr during certain intervals (Pirazzoli and Pluet, 1991). Our

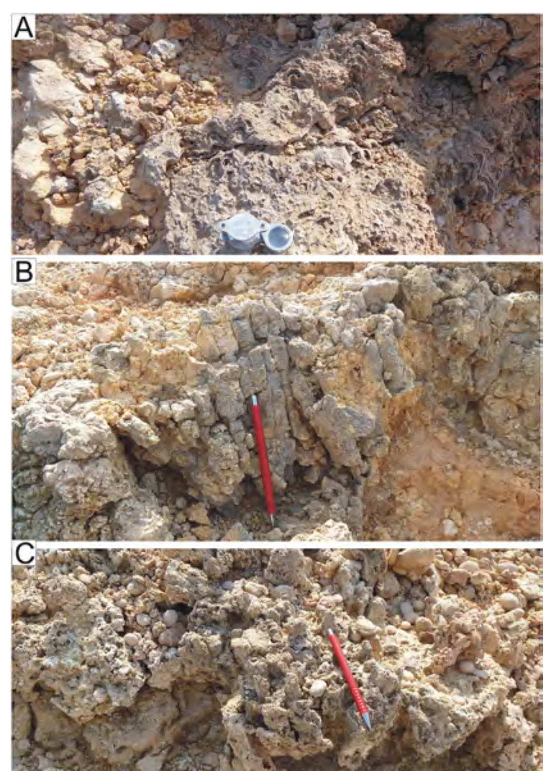

Fig. 7. Different growth forms of coral Cyphastrea serailia. (A) Wavy growth from the protected side of the reef. (B) Columnar growth from the protected side of the reef. (C) Irregular growth form the ocean-facing side of the reef.

quantifications rely on the following considerations.

1. The reefs had formed during the Weichselian (last glaciation) as suggested by (Wyns et al., 1992a; see Introduction!). The age of the corals (21,280 ± 280 yr B.P or 31,110 ± 530 yr B.P.; see introduction!).
2. We consider the post-Weichselian eustatic sea-level rise, which amounted to ~120 m (Pirazzoli and Pluet, 1991).
3. The gentle dip of the reef tops towards the ocean (Fig. 2) resembles that of marine terraces, which are wave-cut platforms. This indicates that the reefs were exposed to erosive effects of waves/breakers, and that the reef's depositional depth was likely close to the sea-level, possibly between 1 and 2 m (1.5 m) and, thus close to shore.
4. The elevation above sea-level of the two reefs is 21.5 m.

The overall or cumulative uplift of the reefs is an addition of the post-Weichselian sea-level rise (~120 m), the depositional depth of the reefs (1.5 m) and their present elevation above sea-level (21.5 m) and amounts to 143 m. The annual uplift rate is determined by dividing the uplift (143 m) by the age of the reef before the Holocene (~21,000 or ~31,000 yr B.P.) and amounts to 6.8 or 4.6 mm/yr, respectively.

5. Interpretation

Besides the uplifted reefs of the “Qmy unit” and the abrasion platform we found additional and independent field evidence for uplift that affected this unit: (1) beach conglomerate 1 overlying and postdating reef formation, (2) the raised wave-cut notch and (3) beach conglomerate 2 cemented onto the notch, postdating notch formation. Further evidence for uplift is provided by microscopic diagenetic features from the bioclastic limestone and the bafflestone. Equant, drusy cement postdates dissolution (bioclastic limestone) and the first cement (bafflestone). This reflects the transition from the phreatic marine environment (first cement) to vadose meteoric conditions (dissolution and precipitation of equant, drusy cement).

Since wave-cut notches and beach conglomerates generally form at sea-level, their depositional depths was slightly shallower than that of the reefs. Stratigraphically, we found the wave-cut notch in the bioclastic limestone and, thus, below the reefs. Formation of beach conglomerate 1, which accumulated on top of the reef, is related to uplift of the abrasion platform following reef formation. Formation of beach conglomerate 2, which is associated with the notch, postdates deposition of conglomerate 1 as the latter occupies a more elevated position. Both conglomerate denote periods of uplift towards shallower waters and possibly to meteoric conditions. Conglomerate 2 deposition ensued close to a wadi estuary which points to the meteoric influence (or mixed meteoric and marine influence) of the clastic material following notch formation.

The notch we observed was not entirely formed by wave action as indicated by the borings. Evidently, notch formation is related to both bioerosion (Fig. 3B) and wave induced erosion during periods of relative stable climatic conditions (Cooper et al., 2007).

Hardground formation is commonly associated with sedimentary hiatuses and flooding events (e.g., Fürsich et al., 1992; Pope and Read, 1997). The hardground shown in Fig. 4A is an upper bedding surface and a wave-cut/abrasion platform at the same time. Taking into account that abrasion of the platform and also the creation of the borings require time and also considering the global post-Weichselian sea-level rise, we suggest that the hardground found in the bioclastic limestone is associated with an interval of relatively slow uplift and tectonically and climatically (sea-level!) stable conditions. We put forward the idea that the abrasion platform formed before the last glaciation maximum (>20 ka), considering that during the time prior to the last glaciation maximum (30,000–38,000 yr B.P.) the eustatic sea-level was rather stable (Siddall et al., 2003). Fig. 8 depicts formation of the abrasion platform, formation and the notch formation correlated to Marine Isotope Stages (MIS) (Siddall et al., 2003). Coral reef formation may reflect relatively stable tectonic conditions and a stable sea-level following formation of the abrasion platform. The abrasion platform and the reef formed probably during MIS 3 (Fig. 8) which implies that uplift, at least during the last 20,000 yr BP, outpaced the sea-level rise, and which reveals relatively fast tectonic uplift. The common tectonic history for both the abrasion platform and the reef can be envisaged from the gentle dip of the reef tops towards the ocean (Fig. 2) which resembles that of uplifted, wave-cut/abrasion platforms (marine terraces). This indicate that the reefs were exposed to erosive effects of waves/breakers, and that they reflect a depositional depth of about 1.5 m which was close to shore.

Notch formation and the boring into the notch also require some time, and thus, stable tectonic and climatic conditions. Accepting that the notch is younger than the reef, the MIS 1 is a likely candidate for the age of notch formation with a relatively stable sea-level (Fig. 8). We suggest that exposure of the wave-cut notch above sea-level signals an interval of pronounced uplift, possibly associated with faulting and earthquakes.

Provided the age of the reefs was assessed correctly, the uplift of the reefs amounts to 143 m and the annual uplift rate to ~5–~7 mm. Thus, the uplift of studied reefs must have outpaced the post-Weichselian sea-level rise. The causes for uplift are possibly more than twofold. The high relief (~2000 m) in the eastern Oman Mountains less than 10 km west of the study area shows a mechanism of continuous and extensive uplift, probably dating back to early Miocene compression with activation of northwest-striking faults (Fournier et al., 2006; Scharf et al., 2016). Besides Miocene compression, the forebulge interpretation (Ch. 1) as a cause of the uplift sensu Kusky et al. (2005), could have enhanced the uplift rate. In addition, we put forward the idea that uplift can be partly attributed to isostatic rebound following obduction of the dense igneous ophiolite masses and related crustal thickening due to folding and thrusting, considering that the regional topography still reaches an elevation of approximately 3000 m (western Oman Mountains), suggesting crust and mantle are not yet in isostatic equilibrium. Isostatic rebound could be an even more effective uplift mechanism, considering unloading of the crust by intense

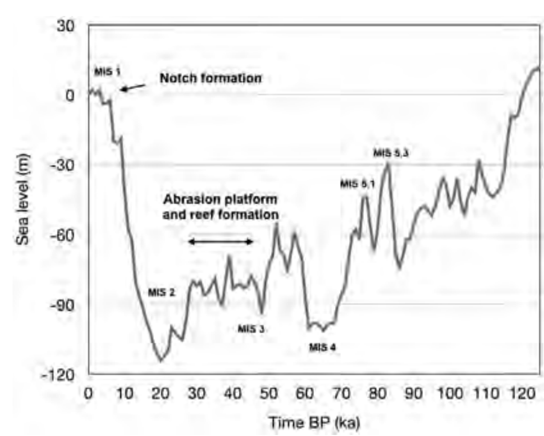

Fig. 8. Platform, reef and notch formation correlated with Marine Isotope Stages (MIS), according to the sea-level data by Siddall et al. (2003). Numbers 1 to 5.2 correspond to different MIS.

erosion of the dense Semail Ophiolite. Large erosional features like the three "dust bowls" of Wadi Mistal, Wadi Sahtan (western Oman Mountains) and Saih Hatat Dome (eastern Oman Mountains) witness the extent of the erosive removal of material.

The importance of the rebound effect as an uplift mechanism has recently gained weight as it was suggested that the forbulge axis had already passed from the study area during the relevant time (Yuan et al., 2016). We found no evidence for subsidence.

6. Summary/conclusions

The reefs are dominated by the coral *Cyphastrea seralia* FORSKÅL 1775 which displays different growth forms. On the protected reef side wavy and columnar structures developed and on the ocean facing side irregularly shaped shapes formed.

The study area represents a setting of multifold dynamic activities at the intersection of hydrosphere, lithosphere and atmosphere. These coastal dynamics include erosional (wave action) and depositional (coral reefs) processes as well an overall eustatic sea-level rise and an overall uplift of the land. Evidently, the uplift outpaced the eustatic Holocene sea-level rise. Uplift of the reefs amounts to 143 m and the annual uplift rate to 6.8 or 4.6 mm/yr.

Interaction/interplay between sea-level rise and uplift was not uniform. Whereas hardground formation, associated with platform abrasion and intense borings reflect relatively slow uplift and tectonically stable conditions, exposure of the wave-cut notch above sea-level signals an interval of pronounced uplift, possibly associated with faulting and earthquakes.

We suggest the following stages of terrace development. (1) The patch reefs formed in shallow water. (2) Gentle uplift caused abrasion of the reef tops. (3) Uplift continued and beach conglomerate 1 was deposited on top of the reefs. (4) Abrasion continued, creating the abrasion platform shown in Fig. 2. Platform abrasion and creation of the borings require some time and an interval of relatively slow uplift and tectonically and climatically stable conditions. The reefs protected parts of the directly underlying bioclastic limestone from erosion, explaining why the reefs are resting on their "pedestals" shown in Fig. 2. (5) During the next stage the wave-cut notch formed below the reefs. (6) Notch formation, including the borings into the notch required time and stable conditions and was followed by deposition of beach conglomerate 2. (7) Finally, emergence/exposure of the notch and conglomerate 2 above sea-level ensued due to pronounced uplift, possibly associated with faulting and earthquakes.

The mechanisms of uplift should be a combination of more than two. Compressional events and forebuldge bending have already been introduced, while the large erosional features in Oman suggest a probable rebound due to intense erosion of the Semail Ophiolite and other rocks.

Acknowledgments

Rocks of the study area have been investigated as part of SQU Final Year Thesis Projects by Al Haddabi (2015) and Al Shukaili (2015). Frank Mattern thankfully acknowledges the paleontological support rendered by Frank Riedel and Annette Kossler (both Freie Universität Berlin), especially during a visit to the reefs in March 2015. We very much appreciate the constructive suggestions by two anonymous reviewers.

References

Aguirre, J., Braga, J.C., Bassi, D., 2017. Rhodoliths and rhodolith beds in the rock record. In: Riosmena-Rodríguez, R.N., Nelson, W., Aguirre, J. (Eds.), Rhodolith/maërl Beds: a Global Perspective. Springer, pp. 105–138.

Al Haddabi, N.H., 2015. Beachrocks Investigation in Tiwi Area. Final Year Project Thesis. Department of Earth Sciences, Sultan Qaboos University, Oman, p. 32.

Al Shukaili, B.S.H., 2015. Study of Recent-subrecent Fringing Reefs of Fins Area, in Oman. Final Year Project Thesis. Department of Earth Sciences, Sultan Qaboos University, Oman, p. 46.

Béchennec, F., Le Métour, J., Platel, J.P., Roger, J., 1993. Geological Map of the Sultanate of Oman (GIS Version), 1:250,000. Directorate General of Minerals, Oman Ministry of Petroleum and Minerals.

Choquette, P.W., Pray, L.C., 1970. Geologic nomenclature and classification of porosity in sedimentary carbonates. Am. Assoc. Pet. Geol. Bull. 54, 207–244.

Claereboudt, M., 2006. Reef corals and coral reefs of the Gulf of Oman. Oman Historical Association, Muscat, Oman, p. 343, 2006.

Cooper, F.J., Roberts, G.P., Underwood, C.J., 2007. A comparison of 103–105 year uplift rates on the South Alkyonides Fault, central Greece: Holocene climate stability and the formation of coastal notches. Geophys. Res. Lett. 34, L14310. https://doi.org/10.1029/2007GL030673.

Dunham, R.J., 1962. Classification of carbonate rocks according to depositional texture. In: Ham, W.E. (Ed.), Classification of Carbonate Rocks. Am. Assoc. Petrol. Geol. Mem, vol. 1, pp. 108–121.

Embry, A.F., Klovan, J.E., 1971. A late devonian reef tract on northeastern Banks Island. N. W. T Can. Pet. Geol. Bull. 19, 730–781.

Fleitmann, D., Burns, S., Neff, U., Mangini, A., Matter, A., 2003. Changing moisture sources over the last 330,000 years in Northern Oman from fluid-inclusion evidence in speleothems. Quat. Res. 60, 223–232.

Flügel, E., 2010. Microfacies of Carbonate Rocks: Analysis, Interpretation and Application, second ed. Springer Verlag, New York, p. 984.

Fournier, M., Lepvrier, C., Razin, P., Jolivet, L., 2006. Late cretaceous to Paleogene post-obduction extension and subsequent Neogene compression in the Oman Mountains. GeoArabia 4, 17–40.

Fürsich, F.T., Oschmann, W., Singh, I.B., Jaitly, A.K., 1992. Hardgrounds, reworked concretion levels, and condensed horizons in the Jurassic of western India: their significance to basin analysis. J. Geol. Soc. Lond. 149, 313–331.

Gardner, R.A.M., 1988. Aeolianites and marine deposits of the Wahiba sands: character and paleoenvironments. J. Oman Stud. Spec. Rep. 3, 75–94.

Glennie, K.W., Boeuf, M.G.A., Hughes-Clarke, M.W., Moody-Stuart, M., Pilaar, W.F.H., Reinhardt, B.M., 1973. Late Cretaceous nappes in Oman Mountains and their geological evolution. Am. Assoc. Pet. Geol. Bull. 57, 5–27.

Glennie, K.W., Boeuf, M.G.A., Highes-Clarke, M.W., Moody-Stuart, M., Pilaar, W., Reinhardt, B.M., 1974. Geology of the Oman Mountains. Kon. Ned. Geol. Mijnb. Genootsch. Trans. 31 (1), 423.

Glennie, K.W., 2005. The Geology of the Oman Mountains: an Outline of Their Origin, second ed. Scientific Press, Beaconsfield, p. 110.

Goffé, B., Michard, A., Kienast, J.R., LeMer, O., 1988. A case of obduction related high P, low T metamorphism in upper crustal nappes, Arabian continental margin, Oman: P-T paths and kinematic interpretation. Tectonophys 151, 363–386.

Hacker, B.R., Mosenfelder, J.L., Gnos, E., 1996. Rapid emplacement of the Oman ophiolite: thermal and geochronologic constraints. Tectonics 15, 1230–1247.

Hannss, C., 1991. The capital area of northern Oman: basic relief development. Beih. Tüb. Atlas Vord. Orients 31 (1), 130. R. A (Naturwiss.).

Harms, J.C., Chapel, H.N., Francis, D.C., 1984. The Makran coast of Pakistan: its stratigraphy and hydrocarbon potential. In: Haq, B.U., Milliman, J.D. (Eds.), Marine Geology and Oceanography of Arabian Sea and Coastal Pakistan. Van Nostrand Reinhold, pp. 3–26.

Hoffmann, G., Rupprechter, M., Mayrhofer, C., 2013. Review of the long-term coastal evolution of North Oman – subsidence versus uplift. Zeits. Dtsch. Ges. Geowiss. (Germ. J. Geosc.) 164, 237–252.

Kusky, T., Robinson, C., El-Baz, F., 2005. Tertiary-quaternary faulting and uplift in the Oman Hajar Mountains. J. Geol. Soc. Lond. 162, 871–888.

Lippard, S.J., Shelton, A.W., Gass, I.G., 1986. The ophiolite of northern Oman. J. Geol. Soc. Lond. Mem. 11, 178.

Mazzulo, S.J., Anderson-Underwood, K.E., Burke, C.D., Bischoff, W.D., 1992. Holocene coral patch reef ecology and sedimentary architecture, northern Belize, Central America. PALAIOS 7, 591–601.

McCoy, S.J., Kamenos, N.A., 2015. Coralline algae (Rhodophyta) in a changing world: integrating ecological, physiological, and geochemical responses to global change. J. Phycol. 51, 6–24.

Pirazzoli, P.A., Pluet, J., 1991. World atlas of Holocene sea-level changes. Elsevier Oceanogr. Ser. 58, 299.

Pope, M.C., Read, J.F., 1997. High-resolution surface and subsurface sequence stratigraphy of the Middle to Late Ordovician (late Mohawkian-Cincinnatian) foreland basin rocks, Kentucky and Virginia. Am. Am. Assoc. Pet. Geol. Bull. 81, 1866–1893.

Rollinson, H.R., Searle, M.P., Abbasi, I.A., Al-Lazki, A.I., Al Kindi, M.H., 2014. Introduction. In: Rollinson, H.R., Searle, M.P., Abbasi, I.A., Al-Lazki, A.I., Al Kindi, M.H. (Eds.), Tectonic Evolution of the Oman Mountains, vol. 392. Geological Society, London, pp. 1–7 (Special Publication).

Scharf, A., Mattern, F., Al Sadi, S., 2016. Kinematics of post-obduction deformation of the tertiary ridge at Al-Khod village (Muscat area, Oman). SQU J. Sci. 21 (1), 26–40.

Searle, M., 2007. Structural geometry, style and timing of deformation in the Hawasina window, Al Jabal al Akhdar and Saih Hatat culminations, Oman Mountains. GeoArabia 12, 99–130.

Searle, M., Cox, J., 1991. Tectonic setting, origin, and obduction of the Oman ophiolite. Geol. Soc. Am. Bull. 111, 104–122.

Searle, M.P., Malpas, J., 1980. Structure and metamorphism of rocks beneath the

Semail ophiolite of Oman and their significance in ophiolite obduction. Trans. R. Soc. Edinb. 71, 247–262.
Siddall, M., Rohling, E.J., Almogi-Labin, A., Hemleben, Ch, Meischner, D., Schmelzer, I., Smeed, D.A., 2003. Sea-level fluctuations during the last glacial cycle. Nature 423, 853–858.
Short, A.D., 1991. Macro-meso tidal beach morphodynamics. An overview. J. Coast. Res. 7, 417–436.
Trenhaile, A.S., 2000. Modeling the development of wave-cut shore platforms. Mar. Geol. 166, 163–178.
Wiedicke, M., Neben, S., Spiess, V., 2001. Mud volcanoes at the front of the Makran accretionary complex. Pak. Mar. Geol. 172, 57–73.
Wyns, R., Béchennec, F., Le Métour, J., Roger, J., 1992a. Geological Map of Tiwi, Sheet NF 40-8 B, Scale 1:100,000, Explanatory Notes. Directorate General of Minerals, Oman Ministry of Petroleum and Minerals, p. 66.
Wyns, R., Béchennec, F., Le Métour, J., Roger, J., 1992b. Geological Map of Tiwi, Sheet NF 40-8 B, Scale 1:100,000. Directorate General of Minerals, Oman Ministry of Petroleum and Minerals.
Yuan, Y., Kusky, T.M., Rajendran, S., 2016. Tertiary and quaternary marine terraces and planation surfaces of northern Oman: interaction of flexural bulge migration associated with the Arabian-Eurasian collision and Eustatic sea level changes. J. Earth Sci. 27, 955–970.